



LUND UNIVERSITY

Correlation between edge radius of the cBN cutting tool and surface quality in hard turning

Zhao, T.; Agmell, M.; Persson, Johan; Bushlya, V.; Ståhl, J. E.; Zhou, J. M.

Published in:
Journal of Superhard Materials

DOI:
[10.3103/S1063457617040050](https://doi.org/10.3103/S1063457617040050)

2017

Document Version:
Peer reviewed version (aka post-print)

[Link to publication](#)

Citation for published version (APA):
Zhao, T., Agmell, M., Persson, J., Bushlya, V., Ståhl, J. E., & Zhou, J. M. (2017). Correlation between edge radius of the cBN cutting tool and surface quality in hard turning. *Journal of Superhard Materials*, 39(4), 251-258. <https://doi.org/10.3103/S1063457617040050>

Total number of authors:
6

General rights

Unless other specific re-use rights are stated the following general rights apply:
Copyright and moral rights for the publications made accessible in the public portal are retained by the authors and/or other copyright owners and it is a condition of accessing publications that users recognise and abide by the legal requirements associated with these rights.

- Users may download and print one copy of any publication from the public portal for the purpose of private study or research.
- You may not further distribute the material or use it for any profit-making activity or commercial gain
- You may freely distribute the URL identifying the publication in the public portal

Read more about Creative commons licenses: <https://creativecommons.org/licenses/>

Take down policy

If you believe that this document breaches copyright please contact us providing details, and we will remove access to the work immediately and investigate your claim.

LUND UNIVERSITY

PO Box 117
221 00 Lund
+46 46-222 00 00

Correlation between Edge Radius of the cBN Cutting Tool and Surface Quality in Hard Turning

T. Zhao^{a, b}, M. Agmell^a, J. Persson^a, V. Bushlya^a, J. E. Ståhl^a, and J. M. Zhou^{a, *}

^aLund University, Division of Production and Materials Engineering Lund, 221 00, Sweden

^bNorthwestern Polytechnical University, Xi'an 710072, China

*e-mail: jinming.zhou@iprod.lth.se

Abstract—cBN cutting tools with superior mechanical properties are widely used in machining various hard materials. The microgeometry of cBN cutting tools, such as the edge radius, has great influence on the surface quality of components and tool life. For optimized tool geometry, it is crucial to understand the influence of the cBN cutting tool microgeometry on the machined surface quality. In this study, the attempt has been made to investigate the correlation between the cutting tool edge radius and surface quality in terms of the surface roughness and subsurface deformation through a FE simulation and experiment. Machining tests under different machining conditions were also conducted and the surface roughness and subsurface deformation were measured. Surface roughness and subsurface deformation were produced by the cutting tools with different edge radii under various cutting parameters. Both results from the FE simulation and machining tests confirmed that there was a significant influence on the surface quality in terms of both the surface roughness and subsurface quality from the edge radius. There is a critical edge radius of cBN tools in hard turning in terms of surface quality generated.

Keywords: cBN, cutting tool, hard turning, FE simulation, surface integrity.

1. INTRODUCTION

Recently, cBN cutting tools are widely applied in machining various hard materials, for example bearing steels, die steels as well as high speed tool steels, since they possess superior mechanical properties which include high temperature strength, hardness, and high resistance to chemical reactions. It is common that the hard machining with cBN tools is related to finishing operations, in which the performance of the cutting tool is crucial to the final quality of machined parts. In hard turning, the performance of cBN cutting tools can significantly affect the machined quality. The edge geometry of a cutting tool is one of example which may have a crucial influence on the shape of the deformation zone, distribution of temperature and stress over the tool face, and this will further affect changes in the chip flow, surface quality, tool wear, and tool life. As a result, a considerable attention has been focused on the performance of cBN cutting tools as well as the tools microgeometry [1]. Chou et al. [2] investigated the performance and wear behavior of different cBN tools in finish turning. The results show that low cBN content tools consistently perform better than high cBN content counterparts, despite low cBN content tools have inferior mechanical properties. Through the FE simulation and experiment, Zhou et al. [3] found that a correlation between the tool wear and chamfer angle of a cBN tool and the suggested optimized chamfer angle for cBN tool used in finishing hard turning. Tugrul, Ö. et al. [4] studied experimentally the effect of cutting edge geometry and cutting parameters on the surface roughness in finish hard turning of AISI H13 steel and demonstrated the effect of the cutting edge geometry on surface roughness are statistically significant. Caruso et al. [5] performed experiments to investigate the effects of the tool cutting-edge geometry, workpiece hardness, and microstructural changes on the residual stresses. The results show that the tool geometry significantly affects the surface residual stress. Hua et al. [6] analyzed the effect of cutting edge radius and cutting conditions on the residual stress. It is found from the analysis that hone edge plus chamfer cutting edge and aggressive feed rate help to increase both compressive residual stress and penetration depth, and medium hone radius (0.02–0.05 mm) plus chamfer is good for keeping tool temperature and cutting force low. Ventura et al. [7] investigated the influence of customized cutting edge geometries on tool wear performance of cBN tools in interrupted hard turning. The results show that a single chamfered cutting edge is the most appropriate. De Oliveira et al. [8] studied the performance of two grades of

PcBN tools (high cBN and low cBN contents with an added ceramic phase) in the turning of high-chromium white cast iron by evaluating of tool life, wear mechanisms at the tool cutting edges, roughness, and microstructure remaining on the turned surface. The results showed that the grades with low cBN content and the addition of a ceramic phase, the tool life was three times longer than that of the grades with high cBN content.

Besides, the surface quality, as an indicator, is also a very key aspect for evaluating the machined surface and the performance of cutting tools. Therefore, various studies have also concentrated on this issue. Attanasio et al. [9] studied the effect on cutting parameters and tool wear on white layers and dark layers formation in hard turning. The results revealed that cutting parameters and tool wear affect noticeably white and dark layers formation. Boshah et al [10] carried on an investigation of white layer formation for wide range of cutting speeds in hard turning of 54–56 HRC H13 tool steel. The finding suggested that there may not be a direct correlation between white layer formation and wear. Tang et al. [11] carried out experiments to explore the influences of cutting parameters and nose radius on the surface integrity in finish dry hard turning of the hardened tool steel AISI D2. The results revealed that the tiny grooves, severe plastic flow, and extensive material flows at lower feeds have significant influence on the surface integrity. Denkena et al. [12] studied the effect of cutting speed, feed and cutting edge radius on the surface integrity in terms of the surface roughness, residual stress, and microstructure and hardness by summarizing overview to identify the optimal parameter value and improve the endurance of roller bearings. Domenico et al. [13] explored the effects of different cooling conditions on white layer. The results prove that the white layer is partially reduced or can be totally eliminated under the certain process parameters and cryogenic cooling conditions. Choi [14] investigated the influence of the rake angle on the surface integrity and fatigue performance of hard machined surfaces. The results demonstrate that a higher rake angle induces more compressive residual stresses and a more softened layer, and the rake angle has a significant influence on the fatigue life and that the effect is further increased if the loading is reduced.

Apparently, numerous researches have been carried out. But handful researchers have been attracted by the effect of edge radius on subsurface deformation. In this paper, an attempt has been made to explore the effect of edge radius on the surface roughness and subsurface deformation in hard turning of hardened bearing steel AISI52100. A numerical model was also used to analyze the effect of edge radius in metal cutting. Meanwhile, the experiments were conducted at three groups of edge radii of 20, 30, 40 μm . Through combining the simulation and experiments, the correlation between edge radius of the cBN cutting tool and surface quality was investigated.

2. EFFECT OF CUTTING TOOL EDGE RADIUS

Edge radius is commonly prepared for the cBN cutting tool to enhance the strength of the cutting edge and increase the tool life for its brittleness in the property, particularly in the case of intermittent cut of hard turning, where the high impact cutting force can deteriorate the sharp cutting edge very rapidly. The edge radius in the cutting tool can also change the mechanism of the cutting process, since the edge radius will affect the position of stagnation in the metal removal process and the different stagnation positions may affect the cutting forces and surface quality. The understanding of the edge radius effect on the surface quality is obviously essential in hard turning process for optimization of the cutting tool and process parameters. The schematic relationship between the cutting edge radius and stagnation is shown in Fig. 1. As it can be seen, the stagnation point P is the location, at which the shear stress on the cutting tool is close to zero, and the material flow separation occurs at this point. Upper part of a workpiece material is forming the chip and the other part under the cutting tool is becoming the machined surface. The point S is the position where the cutting tool departs from the machined surface. The height of the stagnation point, y_s , is defined as the distance from the P point to the S point in the axial direction.

A thermally coupled FE-analysis of a cutting process was performed with an updated-Lagrangian formulation and an implicit time integration scheme. The elements used for this analysis were a 3-node plane strain thermally coupled triangle, linear displacement, and temperature (CPE3T in Abaqus). The physical properties of both the workpiece material and the tool material are shown in Fig. 2. The flow stress of the workpiece material was modelled with Johnson-Cook, developed by Johnson [15]. The interaction was modeled with a combined Coulomb and stick friction model according to

$$\tau_f = \min(\mu\sigma_n, \tau_{\max}), \quad (1)$$

where τ_f is the frictional shear stress, μ is the friction coefficient, σ_n is the normal stress, and τ_{max} is the shear strength of the workpiece material, defined as $\tau_{max} = \frac{\sigma_y}{\sqrt{3}}$. The friction coefficient at the contact interface is set to 0.35, which is adopted by [16].

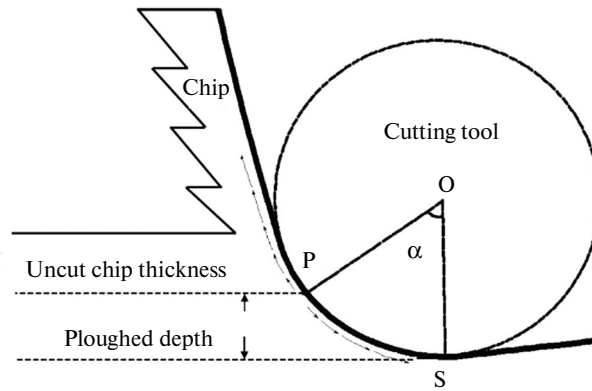


Fig. 1. Schematic view of the shear forces acting on the cutting tool at the stagnation zone.

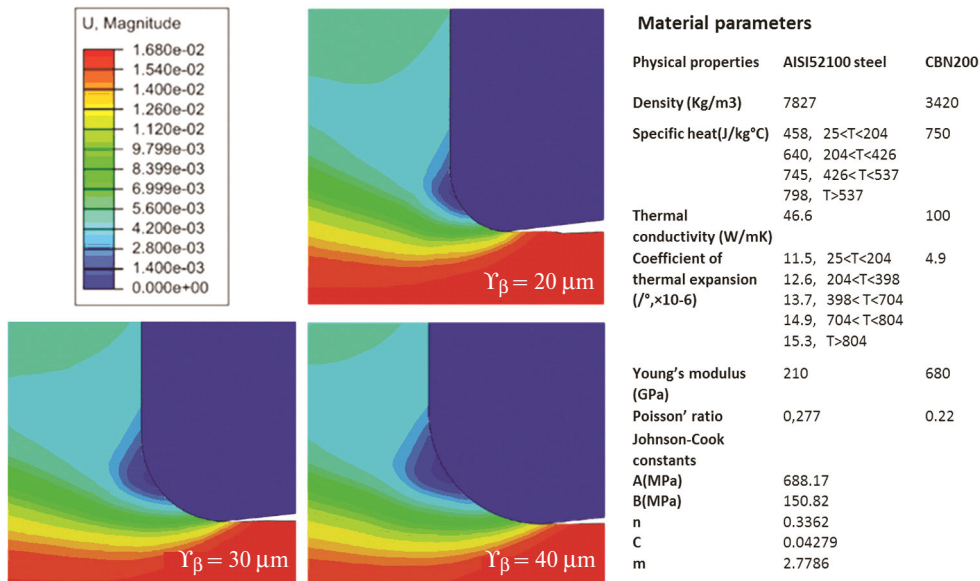


Fig. 2. The material flow of workpiece at three different edges radii.

The cutting tool had a clearance angle, α of 6° , a rake angle, γ of 0° , and three different edge radii r_β of 20, 30, 40 μm . The cutting speed was set to 120 m/min. Three simulations were performed with an uncut chip thickness, h_1 equal to 0.2 for each edge radius.

After the FEM simulation, the material flow of the workpiece material of the three different edge radii is presented in Fig. 2, where the field illustrates the node displacements in the workpiece. It can be noted that the stagnation zone seems to develop closer to the rake face for a smaller edge radius. The axial shear force component acting on the tool is shown in Fig. 3, the change in the direction of the axial shear force indicates the location of the stagnation point, y_s . From Fig. 3 it also can be found that the stagnation zone is closer to the rake face when the cutting tool is with smaller edge radius.

3. MACHINING TEST

The workpiece material used in this study was AISI 52100 alloy steel in the bar shape of diameter 50 mm and 150 mm in length. The hardness of the workpiece is in the 53–58 HRC range. The composition of the workpiece material is shown in Table 1 [17, 18].

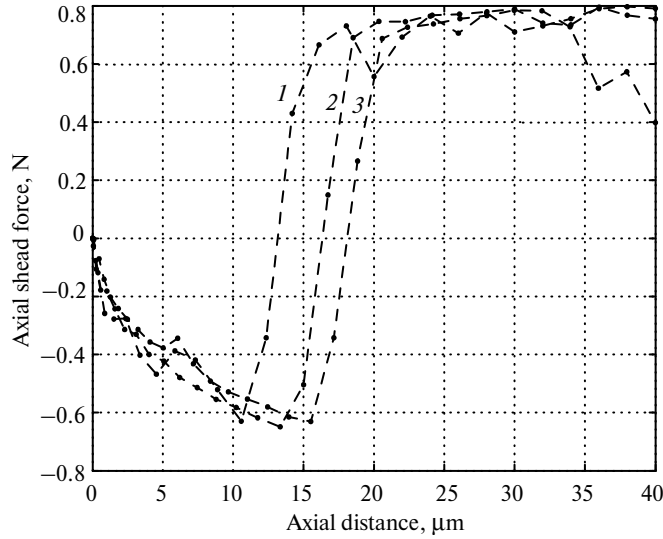


Fig. 3. Axial frictional force component acting on three different edge radii: $r_{\beta} = 20$ (1), 30 (2), 40 (3) μm .

Table 1. Chemical composition of the AISI 52100 workpiece material

C	Si	M_n	P	S	Cr	Al	Cu	Fe
0.95–1.05	0.15–0.35	0.25–0.45	0.025	0.015	1.40–1.65	0.05	0.30	96.9

The cBN cutting tools were used in the test. The tool material contains 85 % cBN with the average grain size of 2 μm . The cutting tool uses a round insert of diameter 9.5 mm and the tool holder is CRSNL3225 which gives the tool geometry of -6° in rake angle and 6° in clearance angle. Before machining experiment, a pre-cut was conducted for each workpiece to remove the rough outer layer remaining from previous process and ensure the surface consistency. Additionally, the workpiece was grooved of width 10 mm to avoid the interaction of different processing parameters. The experiment was performed on the three axial turning lathes. The process parameters are listed in Table. 2.

Table 2. Experimental conditions

Factors	Description
Edge radii r_{β} , μm	20, 30, 40
Cutting speeds v_c , m/min	120, 160, 200
Feed rate f , mm/rev	0.08
Depth of the cut a_p , mm	0.1
Coolant	Dry

4. EFFECT OF THE EDGE RADIUS ON THE SURFACE QUALITY

4.1. Surface Roughness

The surface roughness generated by hard turning process has the characters of anisotropic and periodical in the geometrical structure, as shown in Fig. 4. The anisotropic features include lays and grooves induced by edge chipping and built-up-edge and periodic features include feed marks created by the nose of the cutting tools. This means that the conventional 2D surface roughness, which is computed by functions with one variable ($y = f(x)$) does not enough represent the surface character and 3D surface roughness, which is described by functions with two variables ($z = f(x,y)$) can provide better criteria for the surface roughness. The 3D surface roughness was used to characterize the machined surface. Specifically, the amplitude parameters of S_a and S_k are selected in this study.

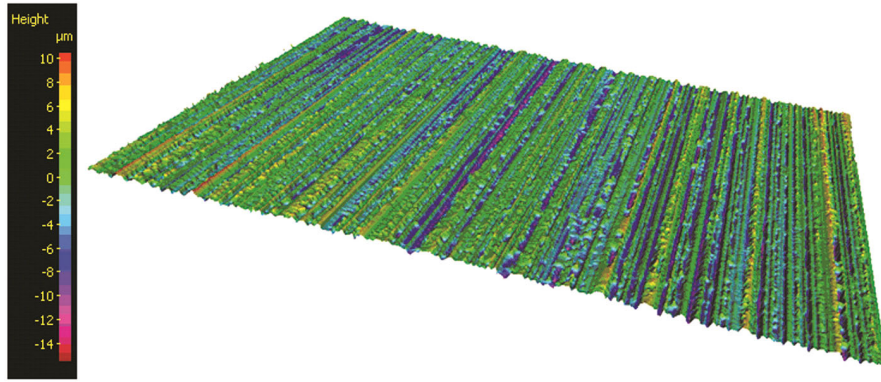


Fig. 4. Typical surface topography measured by Alicona microscope; cutting parameters: $\Upsilon_{\beta} = 20 \mu\text{m}$, $v_c = 160 \text{ m/min}$, $f = 0.08 \text{ mm/rev}$, $a_p = 0.1 \text{ mm}$.

The influence of the edge radius on the roughness of the machined surface in S_a and S_k can be seen in the Figs. 5a and 5b, respectively. It is noticeable that there is an obvious difference respecting S_a and S_k based on different average calculations, but the effect tendency of the edge radius on the surface roughness is basically same. Among three test edge radii, the lowest roughness value of the machined surface was obtained with the edge radius of $30 \mu\text{m}$. The stability of the cutting process could be the major reason for this. The roughness on machined surface produced by the edge radii of 20 and $40 \mu\text{m}$ are higher than the one produced by the edge radius of $30 \mu\text{m}$ in all the tests. The microscope study observed the microgrooves and chip flows on the machined surface, which could attribute to the high roughness value of the surfaces. The cutting speed, however, demonstrated different trends of the influence on the surface roughness. The surface roughness increases with increasing cutting speed except for the edge radius of $40 \mu\text{m}$ at the speed of 200 m/min , in which small vibration was observed during the test.

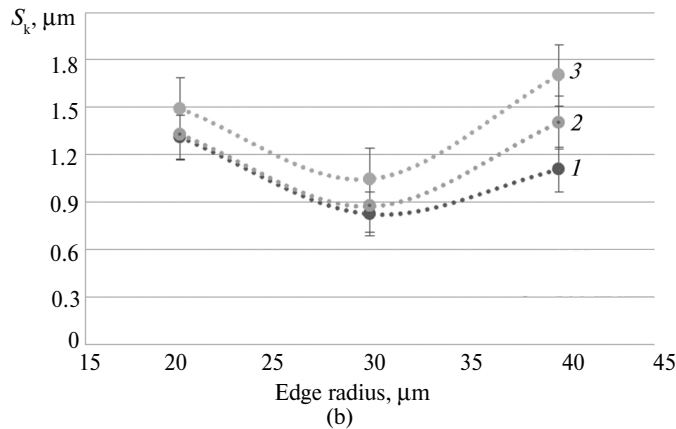
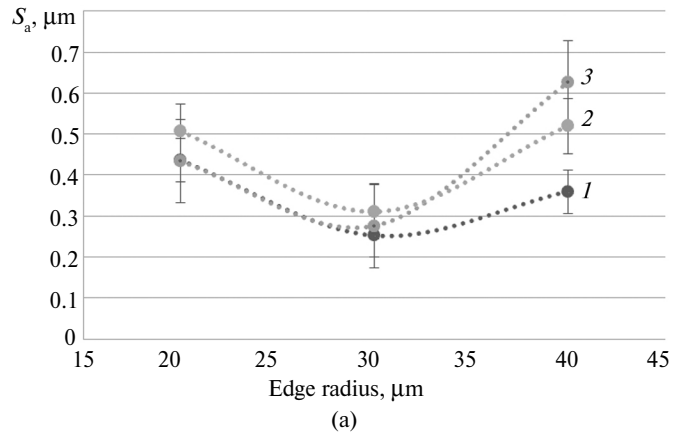


Fig. 5. Effect of edge radius on the surface roughness: 120 (1), 160 (2), 200 (3) m/min.

More statistical features of surface quality can be made with the Abbott-Firestone curves. Figure 6 presents the surface roughness with Abbott-Firestone curves for the surface generated at different cutting parameters. The curves includes three parts, which the peak, core, and valley zone were defined to cover 2–25, 25–75, and 75–98%, respectively. In this study, among the assessing parameters S_{pk} , S_k , and S_{vk} was shown in Fig. 6. The curves basically possess a regular S shape, and the material ratio of valley zone is approximately 90% for all curves owing to the surface texture with grooves. In addition, regarding the evaluating parameters of S_{pk} , S_k and S_{vk} , the value when processed by the edge of 40 μm radius is higher than other experiments, especially much higher than the edge of 30 μm radius. The reason for this is that ploughed depth is greater for a larger edge radius based on the simulation results. Regarding cutting speed, it has same effect on evaluating parameters on this account cutting temperature increases and tool wear increases with increasing cutting speed.

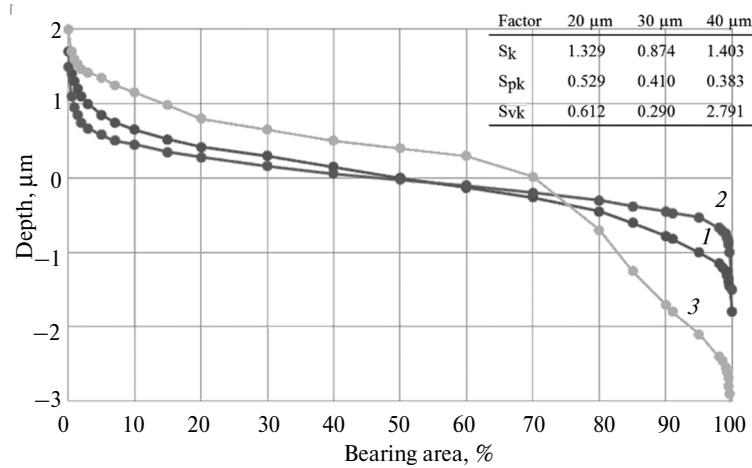


Fig. 6. Abbott-Frestone curves at different turning parameters: 20 (1), 30 (2), 40 (3) μm and 160 m/min.

4.2. Subsurface Deformation

The formation of sub-surface deformation consists mainly of the mechanism of plastic flow, the mechanism of quick heating and quenching and the mechanism of surface reaction, and all these mechanisms may be affected by plastic strain. Therefore, in order to explore the effect of the edge radius on sub-surface deformation, the simulation about the equivalent plastic strain in the sub-surface for different edge radius was carried out, and the results are illustrated in Fig. 7. It can be seen that the width of the deformation layer in the machined surface is affected by change in y_s due to the different edge radiuses. For verifying the results, the sub-surface deformation was measured by Scanning Electron Microscope (SEM) at a magnification of 8000. The surface structures at different cutting parameters are shown in Fig. 8. The machined surface produced with the

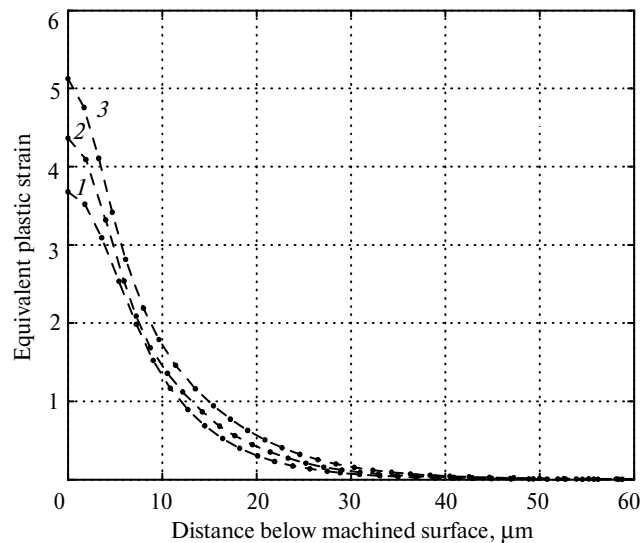


Fig. 7. Equivalent plastic strains in the subsurface for different edge radii: $r_\beta = 20$ (1), 30 (2), 40 (3) μm .

tools in different edge radii are all formed with white layer and severe deformed layer underneath. The thicknesses of white layer and deformation layer were affected by both edge radius and cutting parameters. It was observed from the SEM study that both white layer and deformation layer increase when the edge radius increases and this may attribute to fact that the cutting tool with the large edge radius generated the deeper ploughed depth, which results in the increasing of plastic strain. The results were found to be consistent with the result from FE simulation.

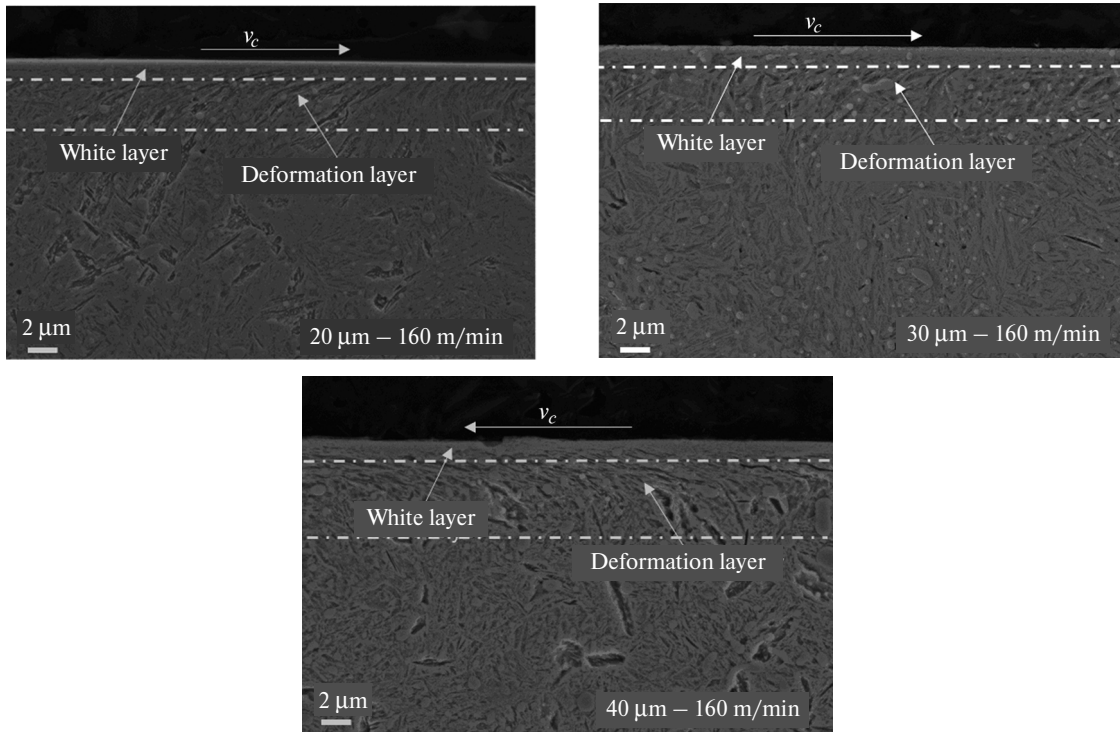


Fig. 8. SEM surface structure at cutting parameters: $v_c = 160$ m/min, $f = 0.08$ mm/ref, $a_p = 0.1$ mm; dry cut; workpiece material—AISI 52100; cutting tool—cBN200.

Figure 9 reveals the influence of the edge radius and cutting speed on the subsurface deformation. Pronounced increase on both thickness of white layer and deformation layer in the machining tests. The thickness of white layer received little influences when tools with edge radius of 20 and 30 μm were used. The influence on thickness of the white layer became substantial when the tool with edge radius of 40 μm was used in the machining and this may primarily related to the increased friction force between cutting edge and machined surface as a result of the large edge radius, see Fig. 9a. This also displayed that cutting speed has same influence on subsurface deformation, see Fig. 9b. The predominant reason for the larger deformation depth at higher cutting speed is attributed to the tool wear and increased temperature at the interface of flank face and machined surface. The higher cutting speed intensified the tool wear and generated higher temperature; thus the bigger subsurface deformation occurred in the machined surface.

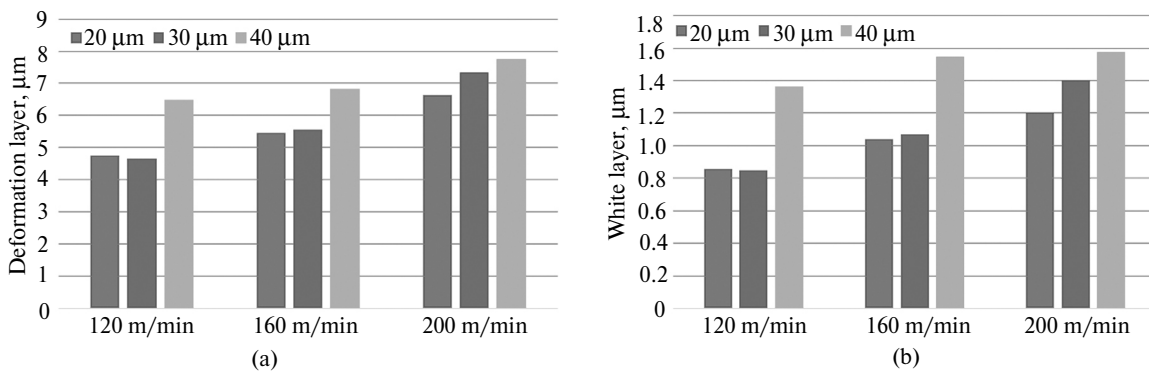


Fig. 9. Effect of the edge radius on the deformation (a) and white (b) layers.

5. CONCLUSIONS

The FEM simulation and machining experiment were used to assess the effect of the edge radii of cBN tools on the surface quality and subsurface deformation in hard turning of bearing steel. The cutting edge radius has a significant effect on the surface roughness and subsurface deformation in hard turning of the AISI52100 steel. Among the three groups of tools, the edge radius of 30 μm exhibits better performance in terms of the surface roughness. The higher surface roughness values were observed in the parts generated by the cutting tool with a larger edge radius. The effect of the edge radius on the subsurface deformation from the FE simulation is confirmed by the machining tests conducted in this study. Both thickness of white layer and deformation layer produced by the cutting tools with three groups of edge radius increase with increase of the edge radius, but substantial increase in the both roughness level, subsurface deformation and white layer was found at the edge radius of 40 μm , which suggests that a cBN tool with the edge radius smaller than 30 μm would be feasible for combination of the edge strength and performance in hard turning.

This research is a part of the strategic research program “the Sustainable Production Initiative, SPI”, cooperation between the Lund University and Chalmers University of Technology. The authors would like to acknowledge Henrik Sandqvist from the SECO Tools AB for supplying the cutting tools in this research. We would also like to thank the financial support from Chinese Scholarship Council (CSC). The research was also co-funded by the European Union’s Horizon 2020 Research and Innovation Programme under Flintstone 2020 project (grant agreement No 689279).

REFERENCES

1. Zhao, T., Zhou, J.M., Bushlya, V., and Ståhl, J.-E., Effect of cutting edge radius on surface roughness and tool wear in hard turning of AISI 52100 steel, *Int. J. Adv. Manuf. Tech.*, 2017, vol. 88, January, pp. 1–8.
2. Chou, Y.K., Evans, C.J., and Barash, M.M., Experimental investigation on cubic boron nitride turning of hardened AISI 52100 steel, *J. Mater. Process. Tech.*, 2003, vol. 134, no. 1, pp. 1–9.
3. Zhou, J.M., Walter, H., Andersson, M., and Ståhl, J.-E., Effect of chamfer angle on wear of PCBN cutting tool, *Int. J. Machine Tools Manuf.*, 2003, vol. 43, pp. 301–305.
4. Özel, T., Hsu, T.K., and Zeren, E., Effects of cutting edge geometry, workpiece hardness, feed rate and cutting speed on surface roughness and forces in finish turning of hardened AISI H13 steel, *Int. J. Adv. Manuf. Tech.*, 2005, vol. 25, nos. 3–4, pp. 262–269.
5. Caruso, S., Umbrello, D., Outeiro, J.C., et al., An experimental investigation of residual stresses in hard machining of AISI 52100 steel, *Procedia Eng.*, 2011, vol. 19, pp. 67–72.
6. Hua, J., Shivpuri, R., Cheng, X., et al., Effect of feed rate, workpiece hardness and cutting edge on subsurface residual stress in the hard turning of bearing steel using chamfer + hone cutting edge geometry, *Mater. Sci. Eng. A*, 2005, vol. 394, no. 1, pp. 238–248.
7. Ventura, C.E.H., Köhler, J., and Denkena, B., Influence of cutting edge geometry on tool wear performance in interrupted hard turning, *J. Manuf. Process*, 2015, vol. 19, pp. 129–134.
8. de Oliveira, A.J., Boing, D., and Schroeter, R.B., Effect of PcBN tool grade and cutting type on hard turning of high-chromium white cast iron, *Int. J. Adv. Manuf. Tech.*, 2016, vol. 82, nos. 5–8, pp. 797–807.
9. Attanasio, A., Umbrello, D., Cappellini, C., Rotella, G., and M’Saoubi, R., Tool wear effects on white and dark layer formation in hard turning of AISI 52100 steel, *J. Wear*, 2012, vol. 286, pp. 98–107.
10. Boshfeh, S.S. and Mativenga, P.T., White layer formation in hard turning of H13 tool steel at high cutting speeds using cBN tooling, *Int. J. Machine Tools Manuf.*, 2006, vol. 46, no. 2, pp. 225–233.
11. Tang, L., Gao, C., Huang, J., Shen, H., and Lin, X., Experimental investigation of surface integrity in finish dry hard turning of hardened tool steel at different hardness levels, *Int. J. Adv. Manuf. Tech.*, 2015, vol. 77, nos. 9–12, pp. 1655–69.
12. Denkena, B., Grove, T., and Maiss, O., Influence of the cutting edge radius on surface integrity in hard turning of roller bearing inner rings, *Production Engineering*, 2015, vol. 9, no. 3, pp. 299–305.
13. Umbrello, D., Analysis of the white layers formed during machining of hardened AISI 52100 steel under dry and cryogenic cooling conditions, *Int. J. Adv. Manuf. Tech.*, 2013, vol. 64, nos. 5–8, pp. 633–642.
14. Choi, Y., Influence of rake angle on surface integrity and fatigue performance of machined surfaces, *Int. J. Fatigue*, 2017, vol. 94, pp. 81–88.
15. Johnson, G.R. and Cook, W.H., A constitutive model and data for metals subjected to large strains, high strain rates and high temperatures, *Proc. 7th Int. Symp. on Ballistics*, The Hague, The Netherlands, 1983, pp. 541–547.
16. Ramesh, A. and Melkote, S.N., Modeling of white layer formation under thermally dominant conditions in orthogonal machining of hardened AISI 52100 steel, *Int. J. Mach. Tools Manuf.*, 2008, vol. 48, no. 3, pp. 402–414.
17. Yakimets, I., Richard, C., Béranger, G., et al., Laser peening processing effect on mechanical and tribological properties of rolling steel 100Cr6, *J. Wear*, 2004, vol. 256, no. 3, pp. 311–320.
18. Galoppi, G. de S., Filho, M.S., and Batalha, G.F., Hard turning of tempered DIN 100Cr6 steel with coated and no coated cBN inserts, *J. Mater. Process. Tech.*, 2006, vol. 179, no 1, pp. 146–153.